

Electron momentum distribution in scandium and the renormalized-free-atom model

T. Paakkari

University of Helsinki, Department of Physics, SF-00170 Helsinki, Finland

K.-F. Berggren and R. Ribberfors

University of Linköping, Department of Physics, S-581 83 Linköping, Sweden

V. Halonen

University of Helsinki, Department of Physics, SF-00170 Helsinki, Finland

(Received 6 October 1975)

The Compton profile of polycrystalline scandium has been measured using 59.54-keV γ rays from a ^{241}Am source. The correction for multiple scattering was calculated and its contribution was found to be $\sim 0.4\%$ at the peak of the Compton profile. Results have been interpreted by means of a renormalized-free-atom model. Good agreement between measured and computed quantities is found if the electronic configuration is chosen as $3d^1 4s^2$ (in atomic notation). Relativistic corrections are studied separately in an Appendix.

I. INTRODUCTION

Several measurements of Compton profiles and the electron momentum densities of $3d$ transition metals have been reported during the last few years. A first series of studies by means of x rays concerns Sc,^{1,2} Ti,³ V,⁴ Cr,⁵ Fe,^{6,7} and Co.⁸ Isotropic Compton profiles for polycrystalline Ti,⁹ V,¹⁰⁻¹² Cr,¹² Fe,^{11,13,14} Ni,^{11,12,15} Cu,^{11,12} and Zn,^{11,12} are now also available from techniques using γ rays. The dependence of the shape of the Compton profile on crystallographic direction has been measured in the case of some transition metals.¹⁵⁻¹⁸

The first attempts to interpret the experimental data theoretically were based on atomic wave functions. Such an approach is evidently not satisfactory since the valence states undergo considerable change in the condensed phase. For this reason the renormalized-free-atom (RFA) model was introduced.¹⁹ It has been found that this still elementary model, in essence a compromise between a purely atomic description and a proper band-structure calculation, can account quite well for the experimentally determined isotropic profiles of Ti,⁹ V,¹⁹ Ni,²⁰ and Cu.²⁰ More recently theoretical profiles have been extracted also from accurate band-structure calculations,²¹⁻²³ and in particular their directional dependence has been studied.^{21,24-26} As regards the comparison between theory and experiments it now seems commonly accepted, however, that good agreement in many cases may be fortuitous. This is because effects of multiple scattering have been neglected in the derivation of Compton profiles from experimental data. Another complicating fact is that the use of γ rays make it necessary to take relativistic effects into account, in particular, for those electrons that are excited in the scattering process into final states with high kinetic energy.^{27,28} Part of the present work is to deal with

these complications.

We shall consider the experimental Compton profile of polycrystalline Sc and its interpretation by means of the RFA model. Scandium was selected in order to complete the experimental study of light transition metals by means of γ rays. In Sec. II the experiments are described and an experimental Compton profile is presented. Effects of multiple scattering are discussed in the same section. The RFA model is briefly described in Sec. III and the corresponding Compton profile is given. A summary is given in Sec. IV. Relativistic corrections in the Compton cross section are considered in the Appendix.

II. EXPERIMENT

Measurements were carried out using the energy dispersive Ge(Li)-spectrometer previously described by Paakkari *et al.*¹⁰ and Manninen *et al.*²⁷ The geometrical divergences of the incident 59.54-keV beam and scattered beam were $\pm 3^\circ$ and $\pm 5^\circ$, respectively. The resolution of the spectrometer was about 0.6 a.u. (full width at half maximum) around 49 keV which corresponds approximately to the energy at the peak of the Compton profile when the scattering angle is equal to 150° .

Scandium foils from two sources were used for preliminary measurements. The nominal purity of both samples was 99.9% but a fluorescent analysis indicated that the thick foil (1 mm) contained considerably more rare-earth impurities (mainly Ce, Pr, Gd, and Dy) than the thin (0.127 mm) foil. Final measurements were made using the thin foil which contained only very small amounts of Pr, Gd, and Dy. The fluorescent radiation from these impurities mainly affects the low-energy side of the Compton profile and all conclusions were made using the high-energy side of the profile. The thick sample and a cold rolled piece of it (0.16 mm)

were used only to study reliability of multiple scattering calculations.

After correcting for background, instrumental resolution, sample absorption, and the energy dependence of the relativistic cross section (cf. Ref. 27 and Appendix for details), the data were converted into an electron momentum scale using the well-known relation

$$p_z = mc \frac{\omega' - \omega + \omega\omega'(1 - \cos\theta)/mc^2}{(\omega^2 + \omega'^2 - 2\omega\omega' \cos\theta)^{1/2}}, \quad (1)$$

where m is the rest mass of the electron, θ is the scattering angle, and ω and ω' are the energies of the incoming and scattered photon, respectively. In Eq. (1) $p_z > 0$ in the high-energy side of the profile and $mc = 137.04$ a.u.

The results obtained for the Compton profile $J(p_z)$ are given in the fifth column in Table I. The high-energy side of the profile is normalized to have an area of 9.4754 electrons from $p_z = 0$ to $p_z = 7$ a.u. This value corresponds to the area under the free-atom profile in the impulse approximation calculated from Clementi's wave functions.²⁹

A. Multiple scattering

A correction for multiple scattering has been done by using a method described in a recent paper,³⁰ where a Monte Carlo program was introduced to calculate the total intensity of twice scattered photons for various experimental situations. The method was applied to the Compton profile of aluminium³¹ to correct the contribution due to the double scattering. For a 0.127-mm-thick scandium sample the ratio of double to single scattering was 1.1% giving an effect of ~0.4% at the peak of the single Compton profile. One can see from Fig. 1 that the main contribution of double scattering lies at $-4.7 \leq p_z \leq 2.9$ a.u. corresponding to a range of energy shifts for scattering from a stationary electron. Thus the corrections due to the double scattering are more prominent on the low-energy side of the profile.

B. Accuracy of results

The principal source of error of the present experiment is the impurity of the sample. On the

TABLE I. Theoretical and experimental Compton profiles of scandium. MS means multiple scattering.

p_z (a.u.)	Free-atom core + $3d^14s^2$	RFA core + $3d^24s^1$	RFA core + $3d^14s^2$	Present Expt.	Present Expt. corrected for MS
0.0	7.657	5.434	5.812	5.794	5.828 ± 0.10
0.1	7.193	5.390	5.769	5.749	5.782
0.2	6.133	5.260	5.638	5.622	5.652
0.3	5.080	5.041	5.420	5.411	5.438
0.4	4.359	4.730	5.111	5.128	5.150
0.5	3.953	4.323	4.710	4.790	4.810
0.6	3.719	3.978	4.216	4.421	4.438
0.7	3.546	3.818	3.628	4.041	4.055
0.8	3.377	3.634	3.433	3.674	3.687
0.9	3.194	3.431	3.243	3.342	3.351
1.0	2.997	3.215	3.042	3.052	3.059 ± 0.06
1.2	2.587	2.772	2.628	2.577	2.580
1.4	2.195	2.349	2.232	2.202	2.202
1.6	1.845	1.997	1.881	1.888	1.885
1.8	1.569	1.669	1.588	1.609	1.604
2.0	1.346	1.424	1.358	1.355	1.349 ± 0.04
2.2	1.176	1.233	1.180	1.164	1.155
2.4	1.042	1.084	1.043	1.032	1.024
2.6	0.938	0.969	0.936	0.937	0.928
2.8	0.856	0.879	0.853	0.869	0.860
3.0	0.786	0.807	0.786	0.795	0.787 ± 0.03
3.5	0.664	0.673	0.663	0.626	0.620
4.0	0.571	0.575	0.570	0.535	0.531
4.5	0.498	0.493	0.491	0.468	0.466
5.0	0.426	0.422	0.421	0.409	0.406 ± 0.02
6.0	0.314	0.308	0.307	0.297	0.295
7.0	0.232	0.224	0.224	0.208	0.208

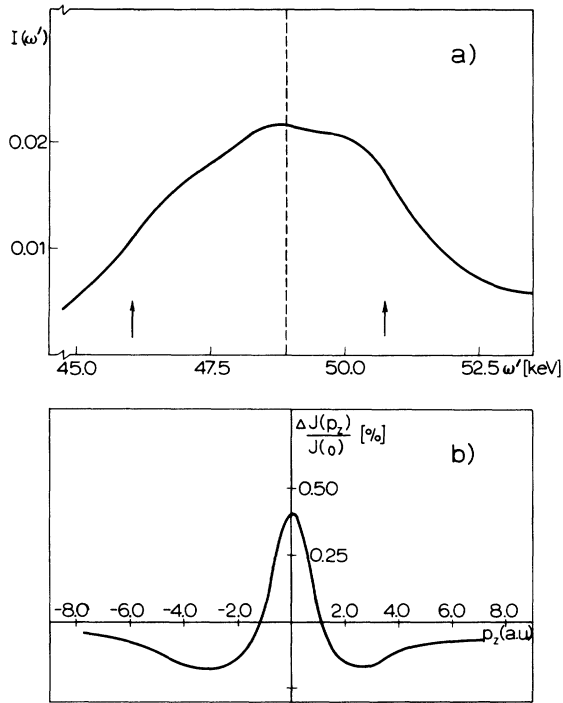


FIG. 1. (a) Spectral distribution of double scattering as a function of energy for scandium with a sample thickness of 0.0127 cm. The arrows indicate the range of energies for scattering from stationary electrons. The broken line indicates the position of the peak of the single profile. (b) Differences between the corrected and uncorrected profiles for the same sample. The correction is given as a percentage of the peak height of the Compton profile. The range of momenta from -4.7 to 2.9 a.u. corresponds to the range of energies for scattering from stationary electrons.

basis of the preliminary measurements and fluorescent analysis the contribution of impurities, mainly Gd $K\beta$, was estimated to be smaller than 1% around $J(0)$ and less elsewhere. The error limits based on the estimated contribution of impurities and on the accuracy of the deconvolution (3σ in Ref. 32) are given in Table I.

III. RENORMALIZED-FREE-ATOM (RFA) MODEL

In the RFA model^{19,33} one utilizes the free-atom Hartree-Fock wave functions, truncates them at the Wigner-Seitz sphere, and renormalizes them to one within this sphere to preserve charge neutrality. The effect of such a truncation is of course largest for the 4s function. Using Clementi's²⁹ atomic wave functions one finds that $\sim 40\%$ of the 4s function is contained in the Wigner-Seitz sphere, which is to be compared with $\sim 95\%$ for the 3d functions. Crystalline effects in the

Compton profile are therefore almost entirely due to the 4s states. Hence it is consistent with present low-resolution type of experiments to ignore renormalization of the 3d states.

The evaluation of the isotropic Compton profile associated with the RFA model has been given elsewhere.^{9,19} We shall therefore give only a few remarks on the construction of the 4s states. It turns out that the truncated 4s atomic function satisfies the Wigner-Seitz boundary condition of a zero derivative at the cell boundary reasonably well. (A simple improvement of the wave function was obtained by putting it equal to a constant beyond its last maximum, but it was later found that the final results were insensitive to such an adjustment.) The renormalized 4s function is thus a reasonable approximation to the true crystal wave function at $k=0$. Other Bloch states in the 4s band are obtained in the usual cell approximation by simply multiplying the RFA wave function by a plane wave. With a spherical Fermi surface this brings in a free-electron-like parabola in the Compton profile at low momenta.

In the calculations we have used Clementi's free-atom wave functions for the $3d^14s^2$ configuration. The lattice parameters of Sc, which forms an hcp structure, were chosen as $a = 3.31$ Å and $c = 5.27$ Å. The configuration of the valence states has been varied and results for the Compton profile are given in Table I and Fig. 2. For an accurate comparison with experiment these profiles have been normalized in the same way as the experimental ones, i.e., a trapezoidal rule was used for the numerical integration over a set of p_z values defined by the experimental results.

IV. SUMMARY

The experimental results are given in Table I together with a free-atom profile calculated for a configuration $3d^14s^2$ from Clementi's wave functions.²⁹ The third and fourth columns give the profiles according to the renormalized-free-atom model with the configuration $3d^24s^1$ (one 4s electron renormalized), and with the configuration $3d^14s^2$ (two 4s electrons renormalized), respectively. It is evident that the present experiment agrees better with the RFA model $3d^14s^2$. To study the origin of the deviations around $p_z = 0.7$ a.u. the theoretical curve (RFA $3d^14s^2$) was convoluted with the residual instrument function as suggested in Ref. 32. The resulting curve is given in Fig. 2 (dashed curve). Although this "theoretical curve" depends on the experimental setup, it gives a more fair comparison with theory. A good agreement is found now also around $p_z = 0.7$ a.u. In other words, a fundamental limitation to detect details of theory with the present experimental

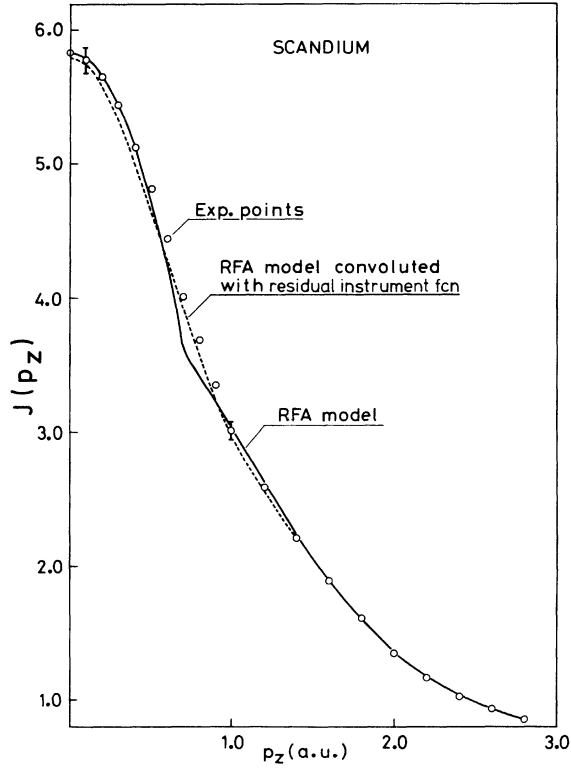


FIG. 2. Compton profile of polycrystalline Sc. The circles denote the experimental results and the bars a statistical error. The full curve refers to the RFA model and the configuration $(3d)^1(4s)^2$. The dashed curve is the RFA model convoluted with the residual instrument function.

resolution is displayed.

Measurements on scandium have also been reported by Manninen¹ and Weiss² but are at variance with present measurements differing by about 10% and -8%, respectively, at $J(0)$.

APPENDIX: RELATIVISTIC CORRECTIONS

In the introduction it was mentioned that relativistic corrections must be considered in the case of γ rays, mainly because the scattered electrons will reach high energies. Manninen *et al.*²⁷ and Eisenberger and Reed²⁸ have considered the following intuitive approach. If binding effects are neglected, the scattering process may be viewed as the scattering of photons from a wave packet consisting of plane wave states. One may then write the total cross section as ($\hbar=c=1$)

$$\sigma = m^2 r_0^2 \int d^3 k' d^3 p' d^3 p \rho(\vec{p}) \frac{1}{2E E' \omega \omega'} \bar{X}(K, K') \times \delta(\pi' + \kappa' - \pi - \kappa), \quad (\text{A1})$$

where $\pi = (\vec{p}, iE)$ and $\kappa = (\vec{k}, i\omega)$ are four vectors de-

fining momenta and energies of the electrons and photons before collision; π' and κ' are the corresponding four vectors after collision. The quantity r_0 is the classical electron radius and $\rho(\vec{p})$ the momentum density of the unperturbed electron system. The \bar{X} factor is defined as

$$\bar{X}(K, K') = K/K' + K'/K + 2m^2(1/K - 1/K') + m^4(1/K - 1/K')^2, \quad (\text{A2})$$

where

$$K = E\omega - \vec{p} \cdot \vec{k}, \quad (\text{A3})$$

$$K' = E\omega' - \vec{p} \cdot \vec{k}' = K + \kappa \cdot \kappa'. \quad (\text{A3}')$$

It should be noted that the flux factor in Eq. (A1) refers to a target system at rest. After integration over final states \vec{p}' and differentiation with respect to ω' and the solid angle Ω' one obtains

$$\frac{d^2\sigma}{d\omega' d\Omega'} = \frac{m^2 r_0^2 \omega'}{2\omega} \int_{p_z} \frac{\bar{X}(K, K')}{E |\vec{k} - \vec{k}'| + p_z(\omega - \omega')} \times \rho(\vec{p}) dp_x dp_y, \quad (\text{A4})$$

where p_z is given by Eq. (1). To extract the Compton profile, defined as

$$J(p_z) = \int_{p_z} \rho(\vec{p}) dp_x dp_y, \quad (\text{A5})$$

from Eq. (A4), is complicated because of the angular-dependent \bar{X} factor. If the scattering angle is $\theta = 180^\circ$, however, \bar{X} becomes a constant. With $E = m$ one hence obtains

$$\frac{d^2\sigma}{d\omega' d\Omega'} = \frac{m^2 r_0^2 \omega'}{2\omega} \frac{\bar{X}(180^\circ)}{m |\vec{k} - \vec{k}'| + p_z(\omega - \omega')} J(p_z). \quad (\text{A6})$$

Previous experimental Compton profiles, as well as the present one, have been deduced from the experimental cross section by means of Eq. (A6) (or slight variations thereof). The experiments are, however, performed with $\theta = 150^\circ$. Below we will justify such a procedure by an explicit calculation for Sc.

It has been shown recently that for an isotropic system the differential cross section can be written³⁴

$$\frac{d^2\sigma}{d\omega' d\Omega'} = \frac{m r_0^2 \omega'}{2\omega |\vec{k} - \vec{k}'|} 2\pi \int_{|p_z|}^{\infty} dp p \rho(p) X_{\text{int}}(p), \quad (\text{A7})$$

where

$$X_{\text{int}} = 2 + F \left(\frac{1}{S'} - \frac{1}{S} \right) + \frac{m^4}{\omega^2} \left(\frac{E-D}{S^3} + \frac{E-D-\omega'(1-\cos\theta)}{S'^3} \right) \quad (\text{A8})$$

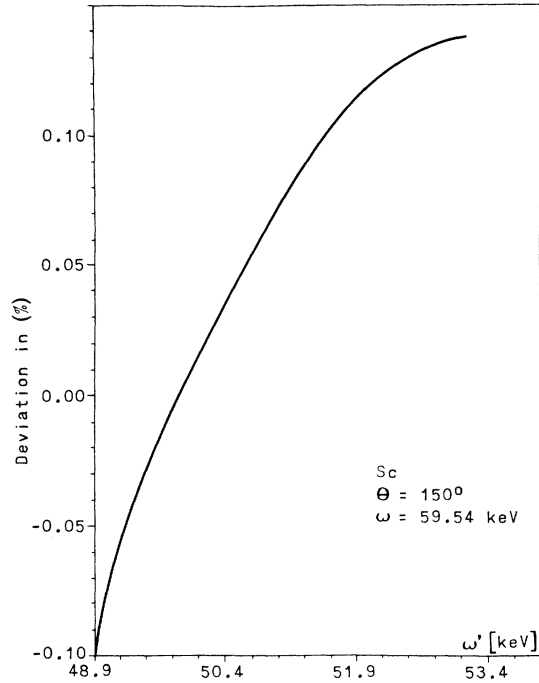


FIG. 3. Deviation in percent from the correct differential cross section for Sc after normalization to the same area in the interval $|p_z| \leq 7$ a.u. The scattering angle is 150° and the energy of the incident radiation is 59.54 keV.

and

$$F = \omega'(1 - \cos\theta) - \frac{2m^2}{\omega} - \frac{2m^4}{\omega^2\omega'(1 - \cos\theta)}, \quad (\text{A9})$$

$$S' = \{[E - \omega'(1 - \cos\theta) - D]^2 - H^2\}^{1/2}, \quad (\text{A10})$$

$$S = [(E - D)^2 - H^2]^{1/2}, \quad (\text{A11})$$

$$D = \frac{(\omega - \omega' \cos\theta)[E(\omega - \omega') - \omega\omega'(1 - \cos\theta)]}{|\vec{k} - \vec{k}'|^2}, \quad (\text{A12})$$

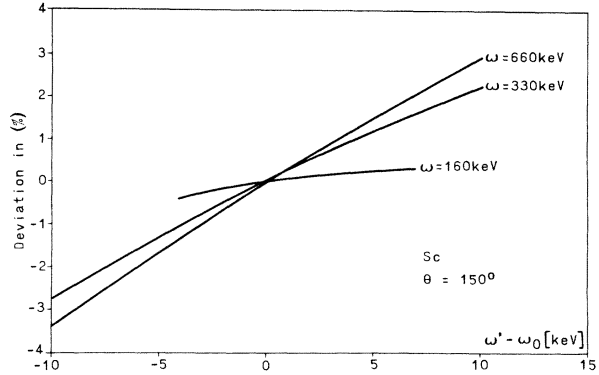


FIG. 4. Deviation in percent from the correct differential cross section for Sc after normalization to the same area in the interval $|p_z| \leq 7$ a.u. The scattering angle is 150° . The frequency of the Compton line is ω_0 .

$$H = (\omega' \sin\theta / |\vec{k} - \vec{k}'|)(p^2 - p_z^2)^{1/2}, \quad (\text{A13})$$

and $E \approx m$. By means of the two different expressions for the differential cross section, Eqs. (A6) and (A7), we have performed numerical calculations for Sc using a momentum density derived from the RFA model. For $\theta = 150^\circ$ and $\omega = 59.54$ keV, which corresponds to the present experiment, the difference between the cross sections is 10% in the interval $|p_z| < 7$ a.u. Although the magnitude of the two cross sections differ they are related to each other by approximately a scaling factor. Normalized to the same area the difference is therefore less than 0.15% as shown in Fig. 3.

In Fig. 4 the difference in the cross sections after renormalization is given for $\omega = 160, 330,$ and 660 keV and $\theta = 150^\circ$. Again it turns out that for $\omega = 160$ keV the deviations are quite small ($< 0.3\%$). For the higher energies, however, the approximation with $\theta = 180^\circ$ in the \bar{X} factor becomes increasingly inaccurate.

¹S. Manninen, J. Phys. F **1**, L60 (1971).

²R. J. Weiss, Philos. Mag. **26**, 761 (1972).

³R. J. Weiss, Phys. Rev. Lett. **24**, 883 (1970); Philos. Mag. **25**, 1511 (1972).

⁴W. C. Phillips, Phys. Rev. B **7**, 1047 (1973).

⁵R. J. Weiss, Philos. Mag. **27**, 1461 (1973).

⁶M. Cooper and B. G. Williams, Philos. Mag. **17**, 1079 (1968). This article reports exploratory measurements on Fe.

⁷W. C. Phillips and R. J. Weiss, Phys. Rev. B **6**, 4213 (1972).

⁸R. J. Weiss, Philos. Mag. **28**, 993 (1973).

⁹K.-F. Berggren, S. Manninen, and T. Paakkari, Phys. Rev. B **8**, 2516 (1973).

¹⁰T. Paakkari, S. Manninen, O. Inkinen, and E. Liukkonen, Phys. Rev. B **6**, 351 (1972).

¹¹W. R. McIntyre (unpublished).

¹²S. Manninen and T. Paakkari, Phys. Fenn. **9**, 129 (1974).

¹³J. Felsteiner, R. Fox, and S. Kahane, Solid State Commun. **9**, 457 (1971).

¹⁴T. Paakkari and S. Manninen, Phys. Rev. B **8**, 3765 (1973).

¹⁵T. Paakkari, P. Suortti, V. Halonen, S. Manninen, Phys. Fenn. **8**, 92 (1973).

¹⁶O. Terasaki, T. Fukamachi, S. Hosoya, and D. Watanabe, Phys. Lett. A **43**, 123 (1973).

¹⁷P. Eisenberger and W. A. Reed, Phys. Rev. B **9**, 3242 (1974).

- ¹⁸S. Wakoh, T. Fukamachi, T. Hosoya, J. Yamashita
J. Phys. Soc. Jpn. 38, 1601 (1975).
- ¹⁹K.-F. Berggren, Phys. Rev. B 6, 2156 (1972).
- ²⁰D. G. Kanhere and R. M. Singru, J. Phys. F 5, 1146
(1975).
- ²¹S. Wakoh and J. Yamashita, J. Phys. Soc. Jpn. 35,
1406 (1973).
- ²²J. Rath, C. S. Wang, R. A. Tawil, and J. Callaway,
Phys. Rev. B 8, 5139 (1973).
- ²³R. M. Singru and P. E. Mijnarends, Phys. Rev. B 9,
2372 (1974).
- ²⁴F. M. Mueller, B. N. Harmon, D. D. Koelling, and
A. J. Freeman, Bull. Am. Phys. Soc. 18, 364 (1973).
- ²⁵C. S. Wang and J. Callaway, Phys. Rev. B 11, 2417
(1975).
- ²⁶J. Yamashita, S. Wakoh, and Y. Kubo, Tenth General
Assembly and International Congress of Crystallo-
graphy, Amsterdam, August 1975 (Collected abstracts)
(unpublished).
- ²⁷S. Manninen, T. Pakkari, and K. Kajantie, Philos. Mag.
29, 167 (1974).
- ²⁸P. Eisenberger and W. A. Reed, Phys. Rev. B 9, 3237
(1974).
- ²⁹E. Clementi, IBM J. Res. Dev. 9, 2 (1965).
- ³⁰B. Williams and V. Halonen, Phys. Fenn. 10, 5 (1975).
- ³¹V. Halonen, B. Williams, and T. Paakkari, Phys. Fenn.
10, 107 (1975).
- ³²P. Paatero, S. Manninen, and T. Paakkari, Philos.
Mag. 30, 1281 (1974).
- ³³L. Hodges, R. E. Watson, and H. Ehrenreich, Phys.
Rev. B 5, 3953 (1972).
- ³⁴R. Ribberfors, Phys. Rev. B 12, 2067 (1975).